Modeling the Seakeeping Performance of Luxury Cruise Ships

Yu Cao[*], Bao-jun Yu and Jian-fang Wang

MARIC-Marine Design & Research Institute of China, Shanghai 200011, China

Abstract: The seakeeping performance of a luxury cruise ship was evaluated during the concept design phase. By comparing numerical predictions based on 3-D linear potential flow theory in the frequency domain with the results of model tests, it was shown that the 3-D method predicted the seakeeping performance of the luxury cruise ship well. Based on the model, the seakeeping features of the luxury cruise ship were analyzed, and then the influence was seen of changes to the primary design parameters (center of gravity, inertial radius, *etc.*). Based on the results, suggestions were proposed to improve the choice of parameters for luxury cruise ships during the concept design phase. They should improve seakeeping performance.

Keywords: luxury cruise ship; seakeeping performance; 3-D linear potential flow theory; frequency domain; design parameters

Article ID: 1671-9433(2010)03-0292-09

1 Introduction

Seakeeping is one of the important performances for a luxury cruise ship. Once the ship has been designed, it is very difficult to optimize the inherent seakeeping performance. Therefore in order to obtain a good seakeeping performance, the ship engineers should carefully consider the ship dimensions, ship lines and other design parameters. In this paper, the seakeeping performances of the luxury cruise ship during concept design phase are studied with model tests and 3-D linear methods in frequency domain (using Hydrostar software). According to the results, the influences of variation of design parameters (center of gravity, inertial radius, *etc.*) are given as suggestions for engineers during concept design phase.

2 3-D linear frequency domain potential flow theory of ship in waves

3-D linear potential flow theory in frequency domain mainly focuses on the research of hydrodynamics and motions of floating bodies in waves with zero forward speed. For example, the research of Faltinsen and Michelsen (1975) and Garrison (1978). With regard to the ship seakeeping prediction with forward speed, engineers introduce the assumption of low forward speed and use zero forward speed Green function to handle the problems, e.g. Beck and Loken (1989) performed the prediction of relative motion using three dimensional pulsating source Green function with zero forward speed.

Assuming the ship travels with mean forward speed U at a certain wave heading in small amplitude of regular wave in infinite water depth. The ship performs the oscillatory motion under the wave force disturbance. We will discuss the hydrodynamic interaction between the wave and ship in the frame of linear potential flow theory. Assuming the interaction between wave and oscillatory ship reaches a periodic state, the unsteady velocity potential around the ship in the body moving coordinate system could be expressed as follows by Dai (1998):

$$\Phi_T(x,y,z,t) = \mathrm{Re}\left[\zeta_a(\phi_0 + \phi_7^0)\mathrm{e}^{\mathrm{i}\omega t} + \sum_{j=1}^{6} \mathrm{i}\omega\eta_j \phi_j^0 \right] \qquad (1)$$

In Eq.(1), ζ_a is the amplitude of regular wave, ω is the encounter frequency of ship with progressive wave, ϕ_0 is the incident wave potential with unit amplitude. ϕ_7^0 is the diffraction wave potential due to the disturbance of ship to incident wave with unit amplitude. η_j $(j=1,2,\cdots,6)$ is the periodical oscillatory displacement component of ship in wave. ϕ_j^0 is the radiation wave potential due to the periodic oscillation of ship with unit amplitude of velocity in the j direction.

At infinite water depth, ϕ_0 can be expressed as follows:

$$\phi_0 = \frac{\mathrm{i}g}{\omega_0} \mathrm{e}^{kz} \mathrm{e}^{-\mathrm{i}k_0(x\cos\beta - y\sin\beta)} \qquad (2)$$

where ω_0 is the circular frequency of incident wave, k_0 is the wave number and $k_0 = \dfrac{\omega_0^2}{g}$ for infinite water depth. β is the encounter wave heading of ship and $\beta = 180°$ is defined as head seas. The encounter frequency ω of ship with the forward speed U can be expressed as: $\omega = \omega_0 - KU\cos\beta$.

η_j can be expressed as follows:

$$\eta_j = \eta_{ja}\mathrm{e}^{i\omega t} \quad (j=1,2,3,\cdots,6) \tag{3}$$

where η_{ja} is the complex amplitude of each oscillatory displacement component.

The formulation of diffraction potential and radiation potential could be expressed as below:
In the domain of fluid:

$$\nabla^2 \varphi_j^0 = 0 \quad (j=1,2,\cdots,7) \tag{4}$$

Linear free surface condition:

$$\frac{\partial \phi_j^0}{\partial z} - \nu \phi_j^0 = 0 \quad (z=0, \nu = \frac{\omega^2}{g}, j=1,2,\cdots,7) \tag{5}$$

Body surface condition:

$$\begin{cases} \dfrac{\partial}{\partial n}\phi_7^0 = -\dfrac{\partial \phi_0}{\partial n} \\[2mm] \dfrac{\partial \phi_j^0}{\partial n} = n_j \quad (j=1,2,\cdots,6) \end{cases} \tag{6}$$

Bottom surface condition:

$$\nabla \phi_j^0 \to 0 \quad (z \to -\infty, j=1,2,3,\cdots,7)$$

Radiation condition:

$$\lim_{R\to\infty}\sqrt{R}(\frac{\partial \phi_j^0}{\partial R} - \mathrm{i}\nu\phi_j^0) = 0 \quad (j=1,2,3,\cdots,7)$$

By using the three dimensional pulsating source Green function $G(p,q)$, the potential could be written as:

$$\varphi_i^0(p) = \iint_S \sigma^{(j)}(q)G(p,q)\mathrm{d}S_q \quad i,j=1,2,\cdots,7 \tag{7}$$

where $\sigma^{(j)}(q)$ is distributed source, $p = p(x,y,z)$ is field point, and $q = q(\xi,\eta,\zeta)$ is source point.

Applying the above body surface conditions, the diffraction potential could be expressed as below:

$$2\pi\sigma^{(7)}(p) + \iint_S \sigma^{(7)}(q)\frac{\partial}{\partial n_p}G(p,q)\mathrm{d}S_q = -\frac{\partial \phi_0}{\partial n_p} \tag{8}$$

The radiation potential could be given as:

$$2\pi\sigma_1^{(i)}(p) + \iint_S \sigma_1^{(j)}(q)\frac{\partial}{\partial n_p}G(p,q)\mathrm{d}S_q = \frac{\partial \phi_i^0}{\partial n_p} = n_i \quad (i,j=1,2\cdots,6) \tag{9}$$

After obtaining the radiation potential ϕ_j, the added mass coefficient and damping coefficient could be given as below:

$$-A_{ij}\ddot{\eta}_j - B_{ij}\dot{\eta}_j = -\rho\iint_S(\ddot{\eta}_j \cdot \phi_j - U\dot{\eta}_j\frac{\partial \phi_j}{\partial x})n_i\mathrm{d}S \quad i,j=1,2,\cdots,6 \tag{10}$$

Diffraction force is given as below:

$$\{F_D(t)\} = \iint_S -\rho\zeta_a(\mathrm{i}\omega - U\frac{\partial}{\partial x})\phi_7\{n_j\}\mathrm{d}s \cdot \mathrm{e}^{\mathrm{i}\omega t} \tag{11}$$

It is also easy to know that incident wave force could be expressed as follows:

$$\{F_I(t)\} = \iint_S p_I(x,y,z)\{n_i\}\mathrm{d}s \cdot \mathrm{e}^{\mathrm{i}\omega t} \tag{12}$$

where $p_I(x,y,z) = \rho g\zeta_a \cdot \mathrm{e}^{kz} \cdot \mathrm{e}^{-ik(x\cos\beta - y\sin\beta)}$ (infinite depth).

Finally the ship motion equation could be expressed as:

$$\sum_{j=1}^6\left\{[(M_{i_j} + A_{ij})\ddot{\eta}_{ja} + B_{ij}\dot{\eta}_{ja} + C_{ij}\eta_{ja}]\right\} = F_I(t) + F_D(t) = F_i^w$$
$$i,j = 1,2,\cdots,6 \tag{13}$$

where M_{ij} is the mass of ship, C_{ij} is restoring coefficient, and F_i is the wave force.

3 The input parameters of model tests and numerical computation

Model tests mainly focused on three conditions: 1) 0 kn forward speed in regular and irregular head wave; 2) 29.5 kn forward speed in regular and irregular head wave; 3) speed 0kn, in regular beam wave, the model scale is 1:80.

Numerical computation is done by Hydrostar software, which is released by BUREAU VERITAS.

Both model tests and numerical computation use the same input parameters. In order to obtain the believable numerical results, the value of the center of gravity, inertial radius and other parameters should be chosen according to the measurement of model. The numerical panel model has 1810 elements as software requested by Chen (2004).

Both model tests and numerical computation mainly consider the pitch motion, heave motion, roll motion and vertical acceleration at bow and stern position. Table 1 presents some of the general design parameter of the luxury cruise ship.

Table 1 Design parameters of luxury cruise ship

Length overall L_{OA}/m	Breadth B/m	Max. deadweight/t	Max. speed/kn
335	38.4	72500	29.5
Length with perpendiculars L_{bp}/m	Max. draught/m	Block coefficient C_B	Cruising speed/kn
296	10	0.62	24

3.1 Roll damping coefficient
In the model test, the free decay experiment was performed at several forward speeds for the roll motion in order to get the roll damping coefficients. The linear plus quadratic speed dependant form was used to fit the free decay curve by William *at al*. (2001).

The non-dimensional roll damping coefficients *a* and *b* of model tests are given as below.

Table 2 Coefficient of model tests

Speed/kn	a	$b/\times10^{-3}$
0	0.166	24.4
24	0.292	5.26
29.5	0.336	8.06

3.2 Wave spectrum and sea states

The following ITTC wave spectrum is used in model test and numerical simulation for the seakeeping evaluation of the luxury cruise ship:

$$S_\zeta(\omega) = \frac{A}{\omega^5} \exp\{-\frac{B}{\omega^4}\}$$

where $A = \frac{173h_{1/3}^2}{T_1^4}$, $B = \frac{691}{T_1^4}$, $h_{1/3} = 4.0\sqrt{m_0}$, $T_1 = 2\pi m_0 / m_1 = 0.7719T_p$.

The sea state numbers used are 4, 5, 6 and 8, the parameters of the sea state are given in Table 3 by Fang (1995).

Table 3 Indication of sea state parameters

Sea state number	Significant wave height $H_{1/3}$/m	Average wave period T_1 /s
4	2.5	6.2
5	4.0	6.8
6	6.0	8.7
8	9.0	10.5

3.3 Non-dimensionalizaion of response parameters

In this paper, the non-dimensional parameters are used as below:

(1) Non-dimensional heave η_{3a} / ζ_a ;

(2) Non-dimensional roll $\eta_{4a} / k\zeta_a$;

(3) Non-dimensional pitch $\eta_{5a} / k\zeta_a$;

(4) Non-dimensional vertical acceleration a_{za} / ζ_a ;

(5) Non-dimensional wave length/ship length λ / L .

The variables in the above parameters are defined as below: ζ_a regular wave amplitude; k wave number; η_{3a} , η_{4a} , η_{5a} heave, roll and pitch motion amplitude; ρ water density; g gravity acceleration; B bread; L ship length between perpendiculars and a_{za} the amplitude of vertical acceleration.

4 The comparison of numerical result with model test data

4.1 The comparison of ship motion in regular head waves

In regular head waves, the numerical responses including response amplitude operator (RAO) of heave, pitch motion and vertical acceleration at bow and stern position were compared with those from the model test results. Figs.1–4 present the comparison at zero forward speed. Figs.5–8 present the comparison at the forward speed of 29.5 kn. In these figures, the scattered points represent the results from model tests. While the solid curve represents the results from the 3-D linear hydrodynamic analysis using Hydrostar software.

It is seen from Figs.1–4 that the numerical results agreed fairly well with the model test data at zero forward speed, and from Figs.5–8 that the vertical motion at forward speed 29.5kn become larger than the corresponding value at zero forward speed condition. The change is caused due to the influence of forward speed on the hydrodynamic performance of ship. At the forward speed case, the numerical results still give very good prediction of the model test data.
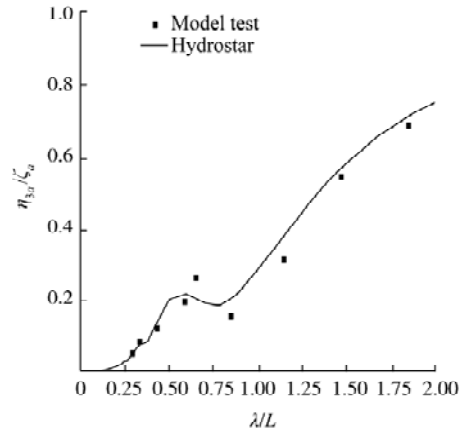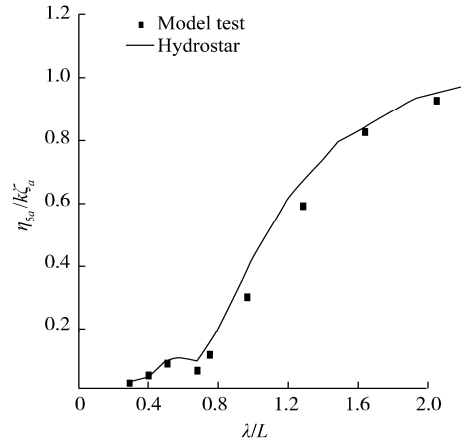

Fig.1 Heave RAO in head wave at 0 kn

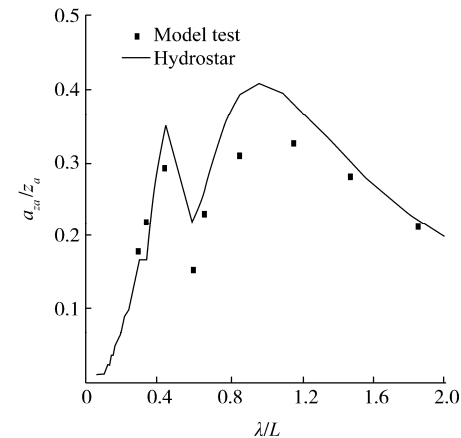**Fig.2 Pitch RAO in head wave at 0 kn**

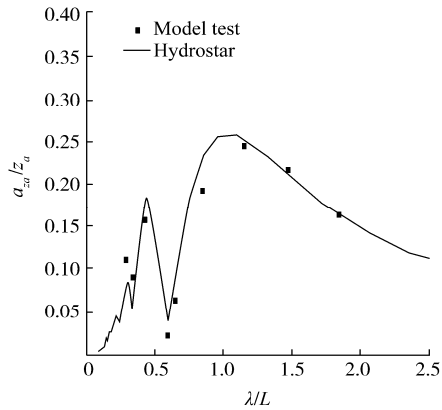**Fig.3 Vertical acceleration RAO at bow position**

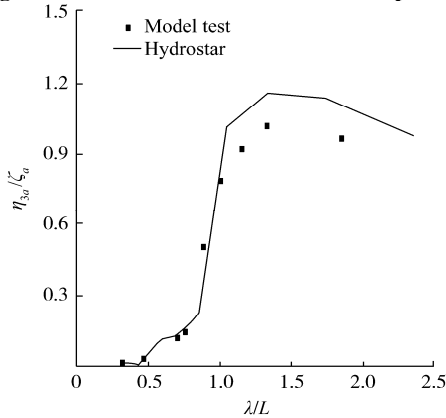**Fig.4 Vertical acceleration RAO at stern position**

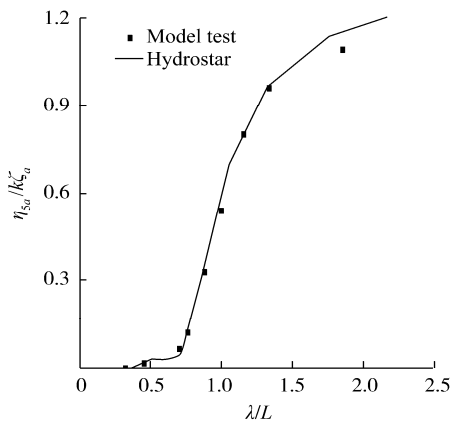
Fig.5 Heave RAO in head wave at 29.5 kn

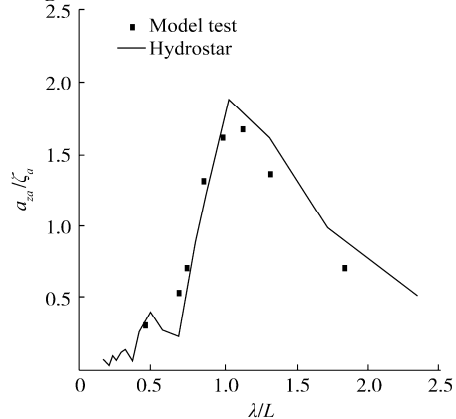**Fig.6 Pitch RAO in head wave at 29.5 kn**

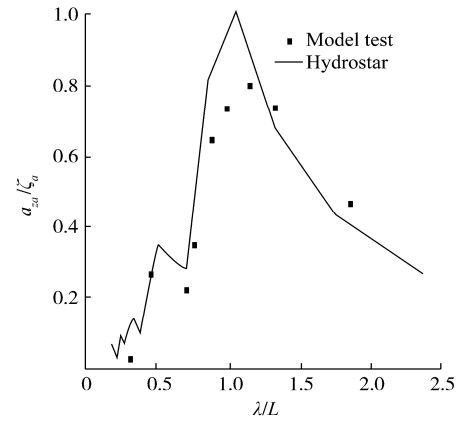**Fig.7 Vertical acceleration RAO at bow position at 29.5 kn**

Fig.8 Vertical acceleration RAO at stern position at 29.5 kn

4.2 The comparison of ship motion in regular beam waves at zero forward speed

Figs.9–12 present the RAO response of roll, heave motion and vertical acceleration at bow and stern positions in beam regular wave at zero forward speed. In the numerical prediction of roll motion using Hydrostar software, the roll damping coefficient in Table 2 obtained from free decay curve of roll motion is used as the roll damping.

It is seen from the comparison that the numerical results show close agreement with the model test data in the beam regular seas at zero forward speed.
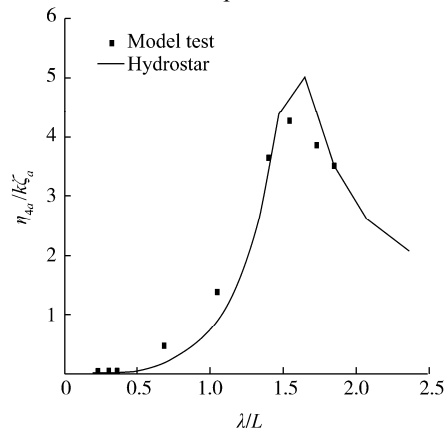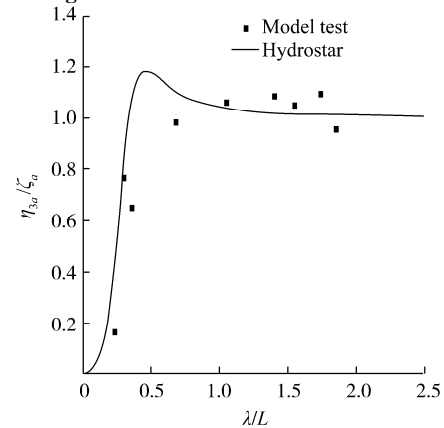

Fig.9 Roll RAO in beam wave at 0 kn
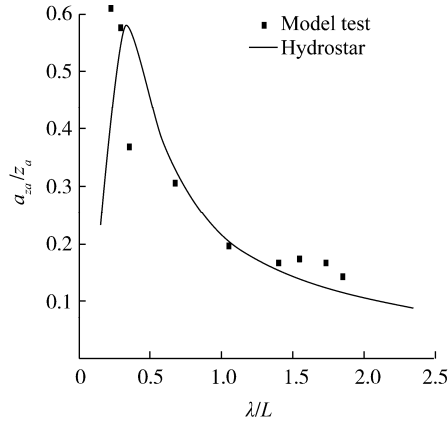

Fig.10 Heave RAO in beam wave at 0 kn

Fig.11 Vertical acceleration RAO at bow position in beam wave
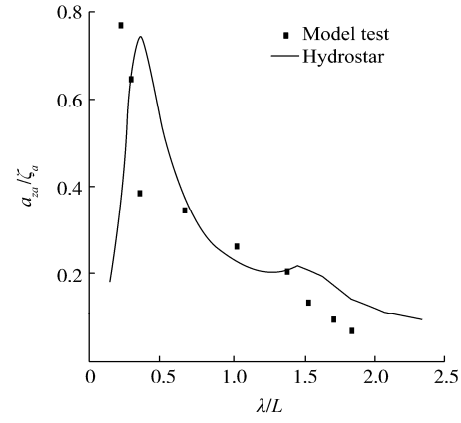

Fig.12 Heave acceleration at stern position in beam wave

Table 4 Significant amplitudes of ship motion at different sea state at 0kn speed

Motion parameter	Sea state 4		Sea state 5		Sea state 6		Sea state 8	
	Model	Num.	Model	Num.	Model	Num.	Model	Num.
Pitch/(°)	0.10	0.12	0.26	0.26	0.68	0.88	1.59	1.94
Heave/m	0.11	0.11	0.18	0.21	0.51	0.54	1.09	1.32
Vertical acceleration at bow position/(m·s^{-2})	0.20	0.21	0.39	0.40	0.74	0.84	1.05	1.44
Vertical accelerationat stern position/(m·s^{-2})	0.11	0.11	0.24	0.20	0.41	0.47	0.75	0.88

Table 5 Significant amplitudes of ship motion at different sea state at 29.5 kn speed

Motion parameter	Sea state 4		Sea state 5		Sea state 6		Sea state 8	
	Model	Num.	Model	Num.	Model	Num.	Model	Num.
Pitch/(°)	0.05	0.04	0.16	0.14	0.81	0.90	2.12	2.34
Heave/m	0.14	0.13	0.17	0.13	0.91	0.97	2.92	3.13
Vertical acceleration at bow position/(m·s^{-2})	0.36	0.40	0.58	0.66	1.84	2.10	4.13	4.79
Vertical acceleration at stern position/(m·s^{-2})	0.46	0.49	0.56	0.61	1.24	1.41	2.27	2.75

4.3 The comparison of ship motion in irregular head wave

Tables 4–5 show the significant amplitude comparison of heave, pitch and vertical acceleration at bow and stern positions in head irregular wave. The ship forward speed is 0kn and 29.5 kn respectively. The sea states are No. 4, 5, 6 and 8 respectively.

It is observed from Tables 4–5 that at sea state No. 4, 5 and 6, the theoretical results agree very well with the model test data. At sea state No.8, the theoretical results are relatively larger than the model test data.

Via the comparison of numerical results of ship motions with the model test data it is seen that the 3-D methods which are used in this paper could predict the luxury cruise ship seakeeping performance in waves under sea scale 8 ($H_{1/3}$=9 m, T_1=10.5) with acceptable engineering accuracy.

5 The investigation of different parameters' influence on seakeeping performance

5.1 The influence of ship speed and wave heading on seakeeping performance

In the following Figs.13–18, the variation of significant

amplitude for pitching, rolling and heave motion with the wave heading and ship speed at sea states 6 and 8 were investigated.

The results are calculated by 3-D methods. In each figure, the ship speed varied at 18, 20, 24, 26 and 29.5 kn, the wave heading varied at 0°, 45°, 90°, 135° and 180°.

Figs.13–18 show that at sea scale 6, the significant pitch amplitude is less than 1.5°, and significant heave amplitude is less than 3 meters, but the maximum significant roll amplitude even reaches 13°. Under the sea scale 8, the significant pitch amplitude is less than 2.8° and the significant heave amplitude is less than 4.7 meters, however the maximum significant roll amplitude even reaches 16°. So, for this kind of luxury cruise ship, we suggest adding the fin stabilizers in order to reduce the roll motion.

At sea state 6, there is rather weak dependence of pitch and heave significant amplitude with regard to the changing of ship speed. For roll motion at 45° wave quartering heading, the roll significant amplitude has a strong dependence on the ship speed, at other wave heading which has rather weak dependence of significant roll amplitude on the changing of ship speed. At sea state 8, there is rather weak dependence

of significant pitch amplitude on the changing of ship speed. Under heave motion at 180° and 135°, there is evident increase of significant value with the increase of ship forward speed, at other wave headings, there is rather weak dependence of significant heave value on the changing of ship speed. The variation rule of significant value of the roll motion with the ship speed is similar to that at sea state 6.

At sea states 6 and 8, there is rather strong dependence of pitch, roll and heave significant amplitude on the changing of wave heading. We suggest finding the best wave heading during sailing in order to obtain the good seakeeping performance of ship.
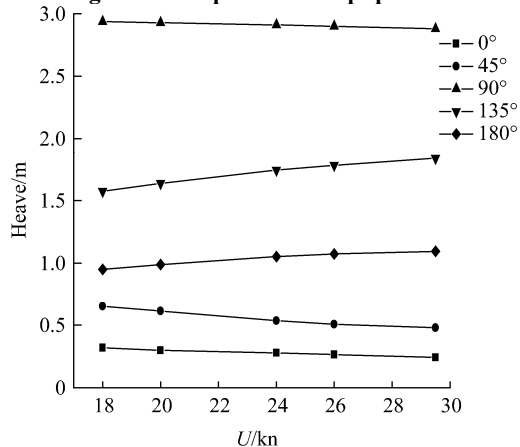

Fig.16 Pitch significant amplitude vs. ship speed at sea state 8
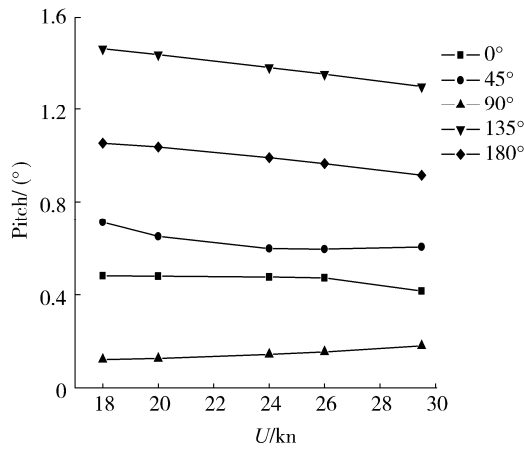
Fig.13 Pitch significant amplitude vs. ship speed at sea state 6
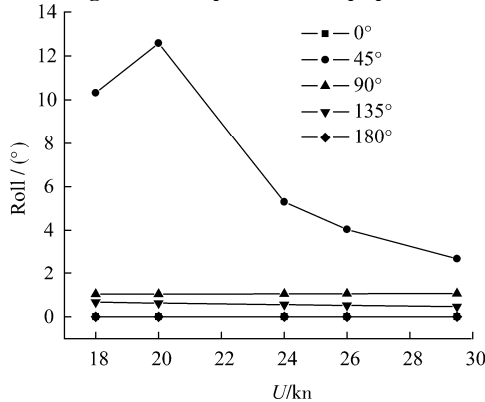
Fig.14 Roll significant amplitude vs. ship speed at sea state 6

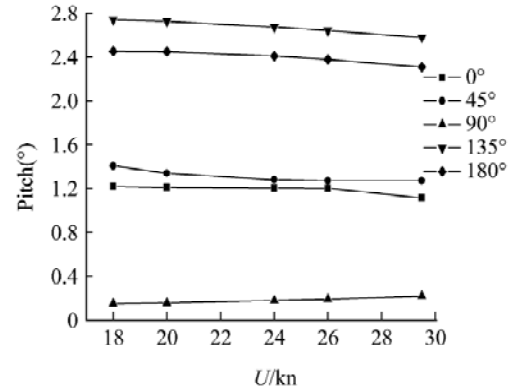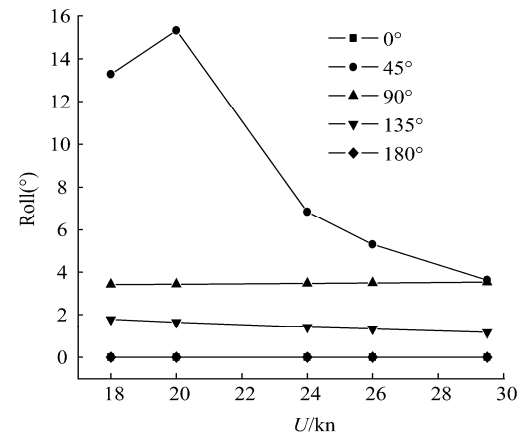**Fig.15 Heave significant amplitude vs. ship speed at sea state 6**

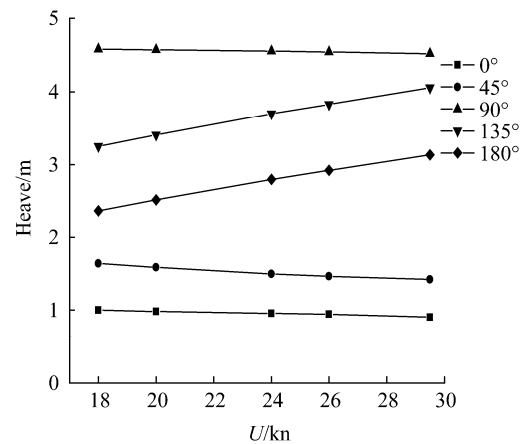**Fig.17 Roll significant amplitude vs. ship speed at sea state 8**

Fig.18 Heave significant amplitude vs. ship speed at sea state 8

5.2 The influence of height for center of gravity on seakeeping performance

Whenever we investigate the influence of different height of center of gravity on ship motions, we found that the variation of the height of center of gravity has evident influence on roll motion, but has neglectable influence on pitch and heave motion. Therefore our study focuses on the relationship of roll motion vs. height of center of gravity in all wave directions.

In Figs.19–22, the initial metacentric height *GM* inertial radius is taken as 2.4 m, 3.0 m and 4.0 m respectively. The variations of significant roll amplitude with the wave heading at sea states 6 and 8 were investigated. The ship speed varied at 24 kn and 29.5 kn respectively, the wave heading varied from following wave to head wave with 15° interval.
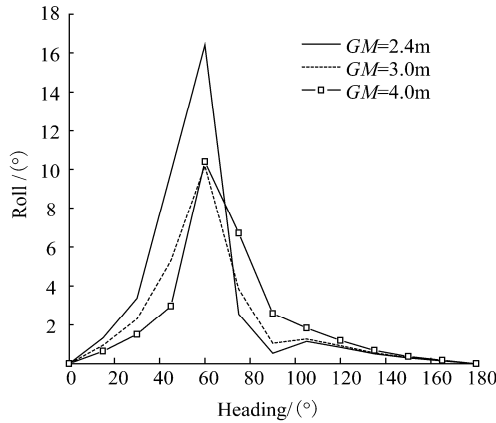

Fig.19 Roll significant amplitude vs. height of center of gravity at 24 kn, under sea state 6
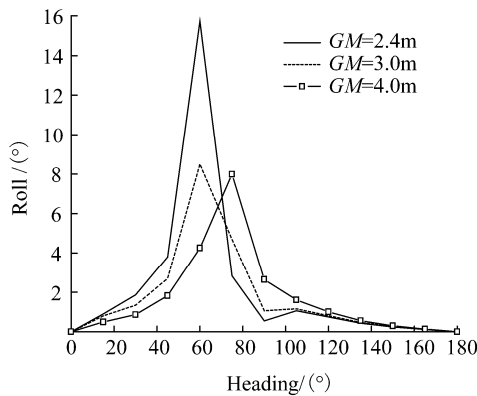

Fig.20 Roll significant amplitude vs. height of center of gravity at 29.5 kn, under sea state 6
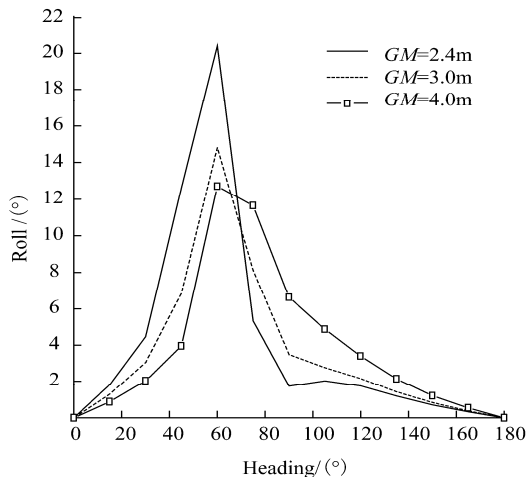

Fig.21 Roll significant amplitude vs. height of center of gravity at 24 kn, under sea state 8
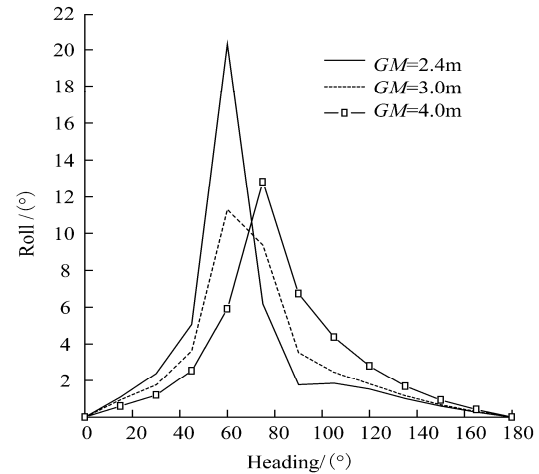

Fig.22 Roll significant amplitude vs. height of center of gravity at 29.5 kn, under sea state 8

Figs.19–22 show a very strong dependence of the maximum roll response on the height for center of gravity. When the initial metacentric height *GM* is 2.4 m, the maximum significant roll amplitude is obviously higher than others.

The maximum significant roll amplitude occurs at quartering seas. So the ship should try to avoid sailing in 45°–60° direction of quartering seas.

Under sea scales 6 and 8 which state at the ship speed of 24kn and 29.5 kn, the roll responses have similar behavior when changing the height for center of gravity. From heading sea 180° to quartering sea 75°, there is an evident increase of significant roll amplitude with the increase of initial metacentric height (decrease of height of center of gravity), which can be fairly demonstrated at beam sea. From quartering seas 45° to following sea 0°, there is an evident decrease of significant roll amplitude with the increase of initial metacentric height (lower height of center of gravity).

Considering seakeeping performance, the luxury cruise ship should sail in all direction waves. But according to the present study, it is better to avoid sailing under 45°–60° direction of quartering seas. From heading sea to some wave heading at quartering sea, the designed ship with the larger initial metacentric height has a higher roll response, and the rule is opposite from quartering sea to following sea. Therefore the height for center of gravity should be moderated to ensure the good seakeeping performance.

5.3 The influence of inertial radius on seakeeping performance

During the investigation of the influence of inertial radius on seakeeping performance, it is demonstrated that the variation of the roll inertial radius significantly influences the roll motion, but the variation of the pitch inertial radius has neglectable influence on pitch and heave motion. Therefore we mainly investigated the relationship of roll

motion vs. height for center of gravity in all wave directions.

In Figs.23–26, the roll inertial radius is taken as 0.35*B*, 0.40*B*, 0.45*B* and 0.5*B* respectively, where *B* represents the maximum hull beam at waterline. The variation of significant roll amplitude with the wave heading at sea states 6 and 8 was investigated. The ship speed varied at 24 kn and 29.5 kn respectively, the wave heading varied from following wave to heading wave with 15 deg interval.

Figs.23–26 show that there is a weak dependence of the maximum significant roll amplitude on changing the roll inertial radius.

At 24 kn forward speed, the maximum significant roll amplitude occurs at quartering seas (45°–60°). From heading sea 180° to quartering sea 60° at which the designed ship with larger inertial radius has smaller roll response. From quartering sea 45° to following sea 0° at which the designed ship with larger inertial radius has higher roll response.
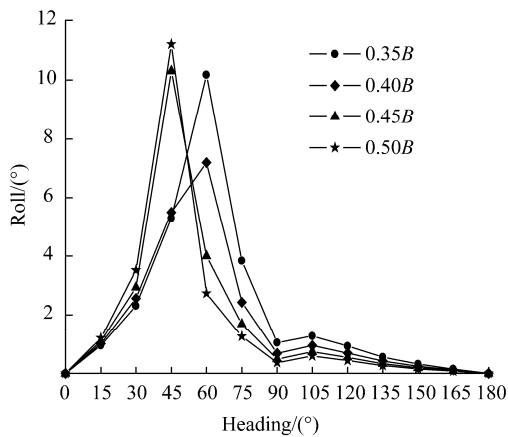

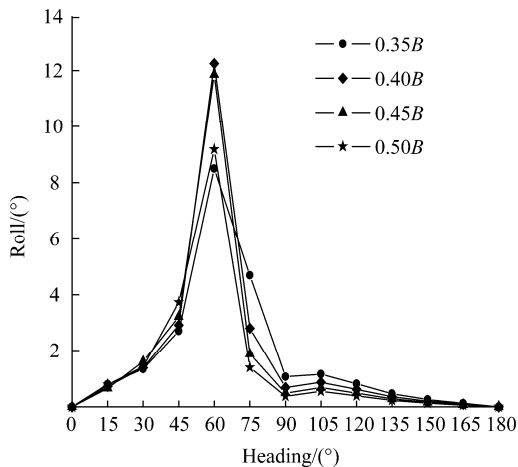**Fig.23 Significant roll amplitude vs. inertial radius under sea state 6 at 24 kn**

Fig.24 Significant roll amplitude vs. inertial radius under sea state 6 at 29.5 kn
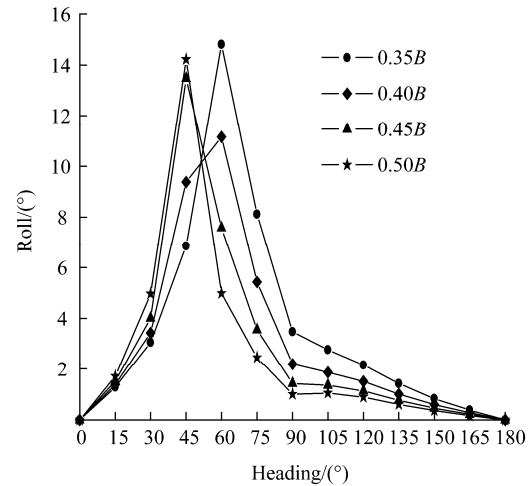

Fig.25 Significant roll amplitude vs. inertial radius under sea state 8 at 24 kn
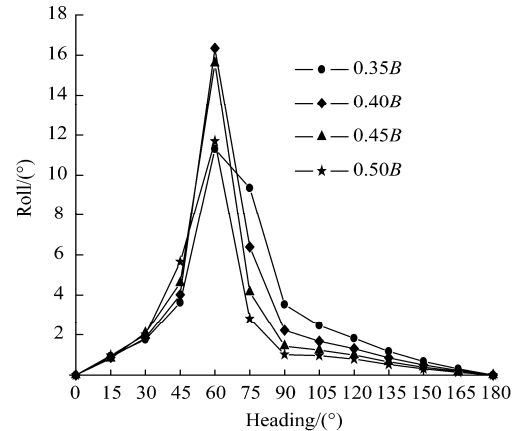

Fig.26 Significant roll amplitude vs. inertial radius under sea state 8 at 29.5 kn

At the ship speed of 29.5 kn, the maximum significant roll amplitude occurs at quartering seas (60°), from heading sea 180° to quartering sea 75° at which the designed ship with larger inertial radius has smaller roll response. From quartering sea 45° to following sea 0° which the designed ship with larger inertial radius has higher roll response.

Considering seakeeping performance, the luxury cruise ship should sail in all direction waves under sea scale 8. But according to the study, it is better to avoid sailing under 45°–60° headings of quartering seas. From heading sea to quartering sea, the designed ship with larger inertial radius has smaller roll response, and the rule is opposite from quartering sea to following sea. Hence the roll inertial radius should be moderated to ensure the good seakeeping performance.

6 Conclusions

According to the comparison of numerical results with model tests, the 3-D method which is used in this paper could predict the luxury cruise ship's seakeeping performance properly.

Through the study, the maximum significant roll amplitude occurs at quartering seas, therefore it is suggested that it is better for ship to avoid sailing under 45°–60° direction of quartering seas and add the fin stabilizers in order to reduce the roll motion. The height for the center of gravity and the roll inertial radius should be moderated to ensure the good seakeeping performance. Via the investigation, it is concluded that the better seakeeping performances of the designers could be achieved by optimization of the design parameters at the beginning of the design stage.

References

Faltinsen OM, Michelsen FC (1975). Motions of large structure in waves at zero Froude number. *International Symposium on the Dynamics of Marine Vehicles and Structures in Waves, Mechanical Engineering*, London, 99-114.

Garrison CJ (1978). Hydrodynamic loading of large offshore structures with three-dimensional source distribution methods. In: *Numerical Methods in Offshore Engineering*, edited by Zienkiewicz OC, A Wiley-Interscience Publication, New York.

Beck RF, Loken K (1989). Three dimensional effects in ship relative motion problems. *Journal of Ship Research*, **33**(4), 261-269.

Dai Yishan (1998). *Potential flow theory of ship motions in waves in frequency and time domain*. National Defense Industry Publication, Beijing, 204-219.

Chen XB (2004). Hydrodynamics in offshore and naval applications-Part 1. *Keynote Lecture of 6th International Conference on Hydrodynamics*, Perth, Australia.

William NF, Marc L, Thomas WT (2001). An investigation of head-sea parametric rolling and its influence on container lashing systems. *SNAME Annual Meeting*, Orlando, 1-24.

Fang Zhongsheng (1995). *Wave statistics for northwest Pacific ocean areas*. National Defense Industry Publication, Beijing, 4-10.

Yu Cao is an engineer of MARIC. His current research interests include hydrodynamics and wave load.

Bao-jun Yu is a professor and naval architect of MARIC. His current research interests include ship overall design and hydrodynamics.

Jian-fang Wang is an engineer of MARIC. Her current research interests include ship overall design and hydrodynamics.